SELECTING RF AMPLIFIERS FOR IMPEDANCE CONTROLLED LLRF SYSTEMS - NONLINEAR EFFECTS AND SYSTEM IMPLICATIONS*

John D. Fox, Themis Mastorides, Claudio Hector Rivetta and Daniel Van Winkle
Stanford Linear Accelerator Center, Stanford CA. USA

Abstract

Several high-current accelerators use feedback techniques in the accelerating RF systems to control the impedances seen by the circulating beam. [1, 2] These Direct and Comb Loop architectures put the high power klystron and LLRF signal processing components inside feedback loops, and the ultimate behavior of the systems depends on the individual sub-component properties. Imperfections and non-idealities in the signal processing leads to reduced effectiveness in the impedance controlled loops. In the PEP-II LLRF systems non-linear effects have been shown to reduce the achievable beam currents, increase low-mode longitudinal growth rates and reduce the margins and stability of the LLRF control loops. We present measurements of the driver amplifiers used in the PEP-II systems, and present measurement techniques needed to quantify the small-signal gain, linearity, transient response and image frequency generation of these amplifiers.

INTRODUCTION

Our previous LLRF studies and simulations stressed the non-linear behavior of the high-power klystron [5].This paper details the testing of a medium power (100W) 476 MHz LLRF amplifier. We now understand that imperfections in these amplifiers are limits to the impedance control achieved in PEP-II, and that without improving these amplifiers the operating current of the LER would be limited to roughly 3100 mA [3, 4].

Figure 1 presents a power spectrum of an LER Klystron output signal during operation at 1900 mA. The obvious central carrier at 476 MHz provides the accelerating fundamental power to the beam. The spectrum also shows revolution harmonics (spaced at +/-n*136 kHz away from the carrier) and small modulations around each revolution harmonic. These modulation signals are very much smaller than the carrier (-60 to -90 dB below the fundamental power), and are providing the necessary signals for the two impedance control loops.

This paper highlights measurements related to communications applications, where two-tone and intermodulation specifications are well defined [6]. The three measurement techniques are:

- Small-signal transfer function (complex frequency response) in presence of a large-signal carrier
- Single sideband image response vs. frequency (large signal carrier, small signal test tone)

*Work supported by Department of Energy contract DE–AC03–76SF00515

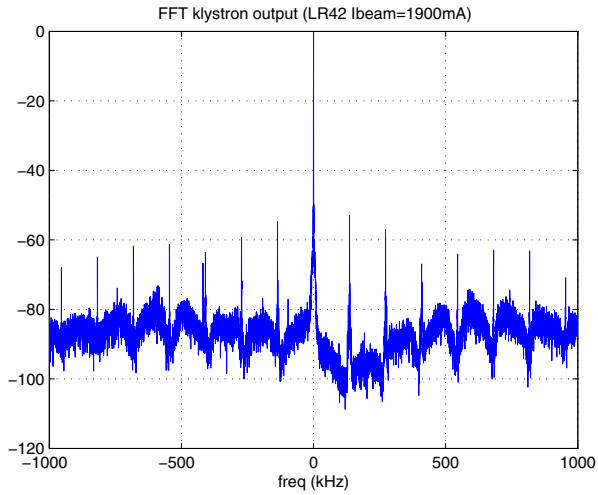

Figure 1: Power Spectrum of LER Klystron Output Power at 1900 mA (center frequency 476 MHz).

- Pulse response- 100% AM modulated RF tone burst

We illustrate each technique with example measurements from Amplifier A (the 120 W amplifier originally specified and commissioned in PEP-II), and amplifiers B and C. In the course of choosing amplifiers we evaluated 5 possible candidates.

SMALL SIGNAL TRANSFER FUNCTION

To characterise the small signal behavior we measure a small signal transfer function in the presence of a large - signal carrier. The carrier signal level is selected to be consistent with the high-power carrier in the actual system, while a network analyzer sweeps across the central operating frequency at levels well below the carrier, typically -30 dB (the IF bandwidth of the analyzer limits how close to the carrier this measurement can be made).

Figure 2 shows large signal and small signal frequency responses for Amplifier A. The no carrier signal response is simply the response of the amplifier swept without the central carrier tone - it shows excellent gain flatness across the band. However, the small-signal measurement reveals a very significant distortion in the frequency response - this variation in gain leads to difficulties in stability of the impedance control loops and reduced effectiveness. More significantly, measuring 11 amplifiers in PEP-II showed significant variation in each amplifier (it was observed that the ”worst” amplifiers were in the ”most difficult to configure” stations). In contrast, responses for two alternate

amplifiers are shown in Figure 3. These alternate amplifiers have similar technical implementation to amplifier A (they are all 120 - 200 W solid state class AB amplifiers) yet these amplifiers have excellent small signal gain uniformity in the presence of the larger carrier.

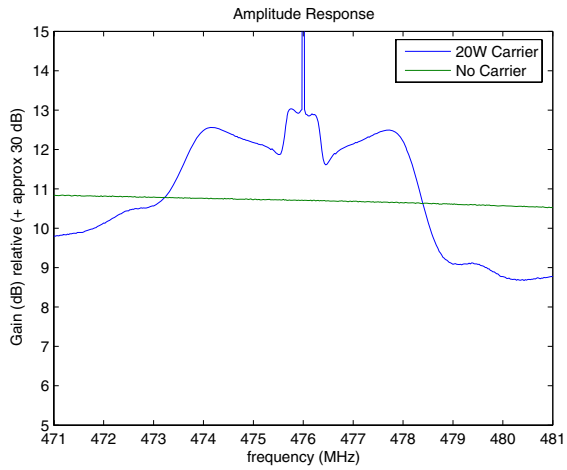

Figure 2: Large and Small-signal Transfer Function measurement of amplifier "A".

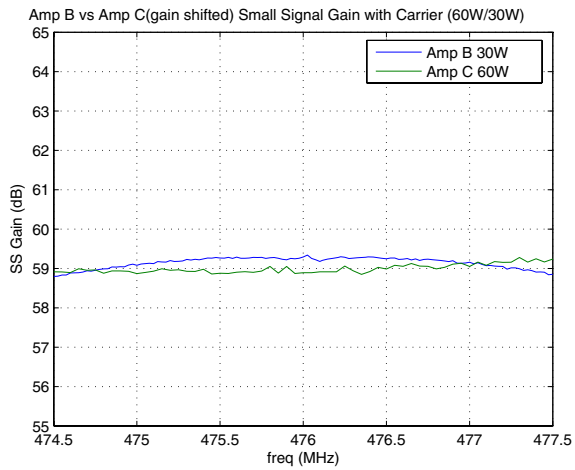

Figure 3: Small-signal Transfer Function measurement of Type B and C amplifiers.

SINGLE SIDEBAND IMAGE RESPONSE

If the amplifier has non-linear response, harmonics of the input excitation are created. If two or more signals are present, nonlinear systems generate a series of intermodulation terms- for input ω_1 and ω_2 the output will contain frequencies at $n*\omega_1+/-m*\omega_2$. For the complicated and rich signals shown in figure 1, many non-linear mixing products can be generated. To quantify the degree of nonlinearity in these LLRF amplifiers, a swept carrier plus single-sideband image test was developed. Here a large signal carrier, and a

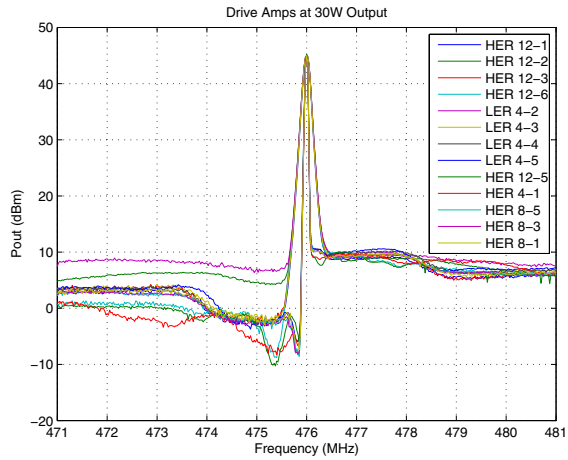

Figure 4: Swept Sideband Image responses for 12 Amplifiers "A".

swept upper sideband tone at a lower level are impressed at the amplifier input - but instead of measuring the response at the excitation sideband frequency, a spectrum analyzer is used to look at maximum power across the band of interest while the excitation sideband signal is swept. A perfectly linear system would display no power at the image frequencies to the left of the center 476 MHz carrier..

Figure 4 shows the responses for 13 of the installed type A amplifiers. Besides the large variations in response between amplifiers, the image signals are roughly -10 to -15 dB below the sideband level (some amplifiers are much worse than this). In the LLRF application, this level of intermodulation would generate interfering signals above and below the 476 MHz fundamental that would transfer modulation from upper to lower revolution harmonics. Figure 5 shows this same sideband test for alternate amplifiers B and C. It is interesting that there is a difference in structure between the amplifiers, but both show better than -25 dB image suppression (for frequencies less than 1 MHz from the carrier one amplifier is clearly better with over -30 dB suppression.

TIME DOMAIN RESPONSES

The third test is a time-domain excitation with 100% AM modulated RF tone bursts at the 476 MHz frequency. While the actual system doesn't run with 100% modulated signals, this test is useful at highlighting the nonlinear behavior of the amplifiers.

Figure 6 shows the time domain responses from amplifier "A"to a 100 ns RF tone burst - the envelope response barely reaches the proper level after 100 ns. This reduced bandwidth for dynamic signals is certainly not suggested by the flat large-signal frequency response shown in figure 2. In comparison, figure 7 shows response for amplifier B.

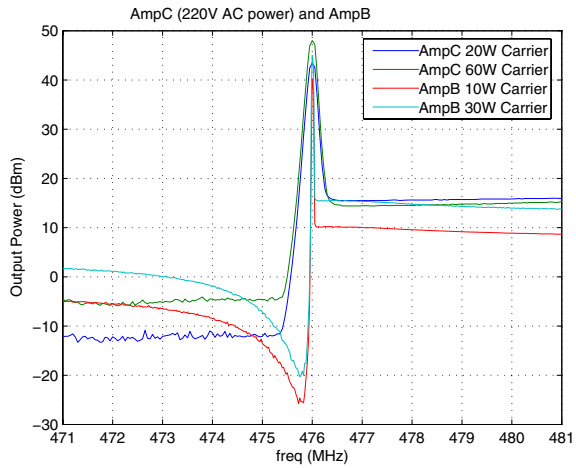

Figure 5: Swept Sideband Image response for Amplifier "B" and "C".

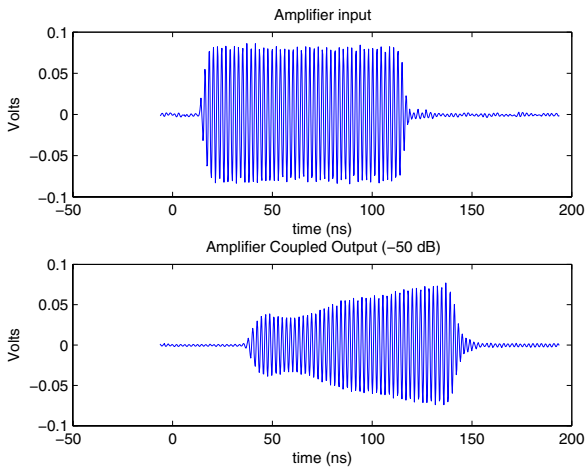

Figure 6: 100 ns RF tone Burst Amplifier "A".

SUMMARY

These simple tests reveal a very complex series of responses, and we can see that no amplifier tested is a perfect linear system. Our modelling effort to understand PEP-II uses the small-signal frequency responses to estimate the loop stability and impedance control of the LLRF systems, and it is clear the frequency response imperfections seen in figure 2 significantly reduce the effectiveness of the impedance control loops [3, 4]. We do not have a direct method to incorporate or quantify the information seen in the sideband rejection and pulse responses, but they are clearly measures of undesired non-linearity.

In selecting new amplifiers for PEP-II, several practical constraints involving the packaging, power supplies, control interfaces, cost and delivery times became involved. For PEP-II we decided to replace all of the LLRF driver amplifiers with a 200W class AB amplifier (the type B amplifier of this paper). As of this conference, 11 of the new

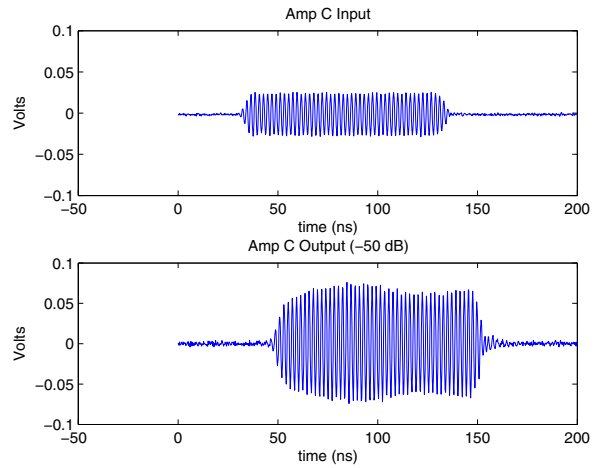

Figure 7: 100 ns RF tone burst Amplifier "B".

amplifiers were installed and commissioned in the HER. We are starting studies in the LER to quantify the closed-loop transfer functions of the stations, and study the difference in growth rates seen with the original and new LLRF driver amplifiers. A subsequent paper will present these results, and compare the data with that from the simulation. One immediate observation is that the closed-loop transfer functions of the RF stations look much less distorted with the new amplifiers, and some historically problematical stations have become much easier to configure and operate than before.

ACKNOWLEDGEMENTS

We thank Phillipe Baudrenghien (CERN), the CERN LLRF group, Heinz Schwarz and Dmitry Teytelman (SLAC) for excellent discussions on these topics. We also thank the PEP-II operations group.

REFERENCES

[1] P. Corredoura, "Architecture and performance of the PEP-II low level RF system," PAC 99, New York, NY SLAC-PUB-8124, Mar 1999. 5pp.

[2] LHC Design Report http://ab-div.web.cern.ch/ab-div/Publications/LHC-DesignReport.html

[3] Claudio Rivetta et. al., "Modeling and Simulation of Longitudinal Dynamics for Low Energy Ring - High Energy Ring at the Positron-Electron Project", Phys. Rev. ST Accel. Beams 10:022801, 2007

[4] T. Mastorides et al., "Analysis of the Longitudinal Low-order Mode Beam Dynamics in PEP-II Rings at High Current Beams", PAC 2007.

[5] D. Van Winkle et al., "Amplitude linearizers for PEP-II 1.2-MW klystrons and LLRF systems." EPAC 06, Edinburgh, Scotland SLAC-PUB-11945, Jun 2006.

[6] Thomas H. Lee, *Planar Microwave Engineering,* Cambridge University Press, 2004